PROCEEDINGS B

rspb.royalsocietypublishing.org

Research

Cite this article: Shirley B, Grohganz M, Bestmann M, Jarochowska E. 2018 Wear, tear and systematic repair: testing models of growth dynamics in conodonts with high-resolution imaging. *Proc. R. Soc. B* **285**: 20181614.
http://dx.doi.org/10.1098/rspb.2018.1614

Received: 18 July 2018
Accepted: 14 August 2018

Subject Category:
Palaeobiology

Subject Areas:
palaeontology, structural biology

Keywords:
vertebrate, teeth, conodont, chordate, growth dynamics, apatite

Author for correspondence:
Bryan Shirley
e-mail: bryan.o.shirley@fau.de

Downloaded from https://royalsocietypublishing.org/ on 09 November 2023

Wear, tear and systematic repair: testing models of growth dynamics in conodonts with high-resolution imaging

Bryan Shirley[1], Madleen Grohganz[1], Michel Bestmann[2] and Emilia Jarochowska[1]

[1]Fachgruppe Paläoumwelt, and [2]Fachgruppe Strukturgeologie, GeoZentrum Nordbayern, Friedrich-Alexander-Universität Erlangen-Nürnberg, Loewenichstr. 28, 91054 Erlangen, Germany

BS, 0000-0002-8532-3890; MG, 0000-0002-2021-2882; EJ, 0000-0001-8937-9405

Conodont elements are the earliest mineralized vertebrate dental tools and the only ones capable of extensive repair. Two models of conodont growth, as well as the presence of a larval stage, have been hypothesized. We analysed normally and pathologically developed elements to test these hypotheses and identified three ontogenetic stages characterized by different anisometric growth and morphology. The distinction of these stages is independently corroborated by differences in tissue strontium (Sr) content. The onset of the last stage is marked by the appearance of wear resulting from mechanical food digestion. At least five episodes of damage and repair could be identified in the normally developed specimen. In the pathological element, function was compromised by the development of abnormal denticles. This development can be reconstructed as addition of new growth centres out of the main growth axis during an episode of renewed growth. Our findings support the model of periodic retraction of elements and addition of new growth centres. Changes in Sr content coincident with distinct morphology and lack of wear in the early life stage indicate that conodonts might have assumed their mature feeding habit of predators or scavengers after an initial larval stage characterized by a different feeding mode.

1. Introduction

Conodonts are an extinct group of vertebrates that flourished within the marine realm from the late Cambrian to Late Triassic. They were the first in this clade to have developed mineralized tissues [1] convergent with those of all other vertebrates [2]. These tissues form phosphatic, tooth-like structures referred to as elements, which were part of the animal's feeding apparatus. Although conodont elements are extremely abundant in marine rocks, it is rare to find soft body remains which are only known from a small number of localities around the world [3,4].

Based on the previous studies of growth allometry [5], microwear [6], ultrastructure [7], finite-element analysis [8,9] and occlusal modelling [8,9], conodont elements are generally accepted to have functioned in a multi-element apparatus of tooth-like structures used for grasping and mechanical digestion of food. Conodont elements consist of basal and crown tissues. In the most derived conodont group, euconodonts, the crown tissue resembles vertebrate tooth enamel in terms of structure and functional adaptations [7]; it is, however, different from vertebrate teeth in that it continued to grow during the life of the animal and underwent repair of fractures and scratches which develop over the course of its life [10,11]. Elements grew by individual episodes of lateral accretion of lamellar tissue [12,13]. The distribution of crown lamellae may thus preserve information on growth dynamics of the animal. Periodicity, or deposition of lamellae in bundles, has been observed in many studies [14–16], which speculated that one lamellae might correspond to a daily increment.

THE ROYAL SOCIETY PUBLISHING

© 2018 The Author(s) Published by the Royal Society. All rights reserved.

Downloaded from https://royalsocietypublishing.org/ on 09 November 2023

Periodic growth is independently supported by the discrete multimodal size distribution observed in large conodont populations [17]. The estimates on the number and relative duration of growth periods vary enormously nonetheless. These differences are exacerbated by the use of disparate protocols, e.g. surface counting of layers at the base of an element does not allow recording of the earliest stages of ontogeny nor episodes of function [15,16]. Observations of etched thin sections are highly susceptible to artefacts and not fully reproducible [14]. As a result, it is not always clear if the same structures are identified as lamellae between studies. Combining the sclero-chronological record provided by lamellae with the distribution of discrete episodes of wear, fractures and subsequent repair [10,11] would allow testing hypotheses on conodont growth dynamics. These episodes are recorded in histological sections and on the surface of the elements, with a distribution consistent with occlusal models informed by other lines of evidence [9]. These episodes have been hypothesized to represent possible periods of mechanical digestion of food, in which sections of tissue were removed at the tip and occlusal side, before re-growing appositionally [11].

Two models of conodont growth addressing the relationships between the elements and their supporting soft tissues have been put forward: (i) growth by the apposition of layers secreted in epidermal pockets, into which the animal retracted the elements during periods of rest [11,14,18]; and (ii) the elements being permanently enveloped in secreting tissue with a 'horny cap' [19,20]. The latter model rejects the retraction of the elements. We test these two models by quantifying the distribution of growth increments in conodonts in combination with the timing and distribution of episodes of function. Studies incorporating the initial phase of conodont growth observed that, in multiple taxa, it is distinguishable in terms of growth dynamics and the resulting morphology [15,16]. This phase has been speculated to correspond to the juvenile (predating sexual maturity) or the larval (predating exogenous feeding) stage. Establishing when conodonts reached sexual maturity may not be possible based on their fossil remains. Here, we test whether the earliest, distinct morphology of conodont elements corresponds to the onset of exogenous feeding by analysing the distribution of wear and damage resulting from food processing, as well as the geochemical composition between the earliest phase and subsequent phases.

We approach these hypotheses using backscatter electron (BSE) imaging which allows us to reconstruct conodont ontogeny quantitatively with a higher resolution and reproducibility than used previously in addressing this problem. Secondly, we use energy-dispersive X-ray spectroscopy (EDX) to propose a reproducible criterion to distinguish individual lamellae and identify changes in the chemical composition between ontogenetic stages.

2. Material and methods

(a) Conodont elements

We selected P_1 elements (for anatomical notation, see [21]) of *Ozarkodina confluens* (Branson and Mehl, 1933) from the middle Silurian of Gotland, Sweden. The normally developed element was collected in the Homerian Halla Formation (*ca* 427.4–430.5 Ma) at the Gothemshammar-9 [22] locality and stored in the collections of GeoZentrum Nordbayern (EJ-14–407-016). The pathological specimen was sampled from L. Jeppsson's collection at the Swedish Museum of Natural History (SMNH, Stockholm) and comes from the Gorstian Hemse Group (*ca* 425.6–427.4 Ma) at Krokvät. It is stored at SMHN under the accession number Co0000038. P_1 elements of *O. confluens* have been selected as a model because their histology has been previously characterized in detail [7,13] and the mechanism of their occlusal has been constrained [11]. Occlusal has been shown to differ drastically between species [23]. Among existing occlusal models, that of *O. confluens* appears to be characterized by the simplest rotational movement, comparable to that documented for the model species *Wurmiella excavata* [8]. This is inferred based on the presence of damage such as spalling and polishing, as well as internal discontinuities, consistently limited in this species to the tips of elements and concentrated in the dorsal part of the blade [8]. This evidence allows constraining of the occlusal surface.

(b) Preparation of conodont sections

The samples were suspended in an epoxy resin (Körapox 398, Kömmerling) and allowed to harden for a period of at least 24 h. The specimens were then ground using a progression of 800 and 1200 grit carborundum (silicon carbide) until the optimal section plane was reached. To finish, they were mechanically (10–20 min, with a progression of 6, 3, 1 µm diamond spray) and chemically polished (OP-S Nondry colloidal silica suspension, 1.5–3 min) using a Logitech WG2 polishing head, before being coated with 3.8 nm of carbon. BSE imaging was conducted using a TESCAN Vega\\XMU scanning electron microscope. As the contrast differences of the internal structures of the conodonts are very small, the contrast amplification was set to a maximum during BSE image acquisition and afterwards again increased with imaging software. Energy-dispersive EDX analysis was conducted using an Oxford Instruments X-MAX 50 mm silicon drift detector, calibrated using silicon or titanium (for 5 KeV and 15 KeV, respectively). One high-resolution transect was measured at 5 KeV, to compare the composition dark and light areas. Changes in composition across the conodont element were measured along three line transects, at a voltage of 15 KeV. All EDX line scans were run for 70–80 min in order to acquire comparable numbers of counts. A Monte Carlo simulation was conducted (Casino v. 3.3) to calculate the interaction volume of the high-resolution transect. The diameter of this was estimated to be *ca* 1.5 µm which may have caused some 'smoothing' of the graph. High-resolution BSE images were pieced together to create a picture of the entire element, in which crown tissue lamellae were counted and their thickness was measured (see data on the Dryad Digital Repository [24]). The widths of dark and light bands were recorded individually at 70 randomly selected points on the conodont element in order to quantify variability in band thickness [24].

(c) Statistical analysis

To test whether there were differences in tissue Strontium (Sr) concentration between growth stages, two mixed-effects models have been fitted to Sr counts from three transects measured across the entire element (figure 3) using the lme4 package [25] and the R software 3.5.0. A null model has been fitted, considering only three transects as a random effect. This model was tested against: (i) a model taking into account transects as a random effect and growth stages as a fixed effect, (ii) a model with occlusal versus non-occlusal side as a fixed effect and transects as a random effect, and (iii) a full model incorporating all the above parameters. Considering that the core of the studied element consists of a different tissue (white matter, figure 3) and may not be comparable with the lamellar tissue

Downloaded from https://royalsocietypublishing.org/ on 09 November 2023

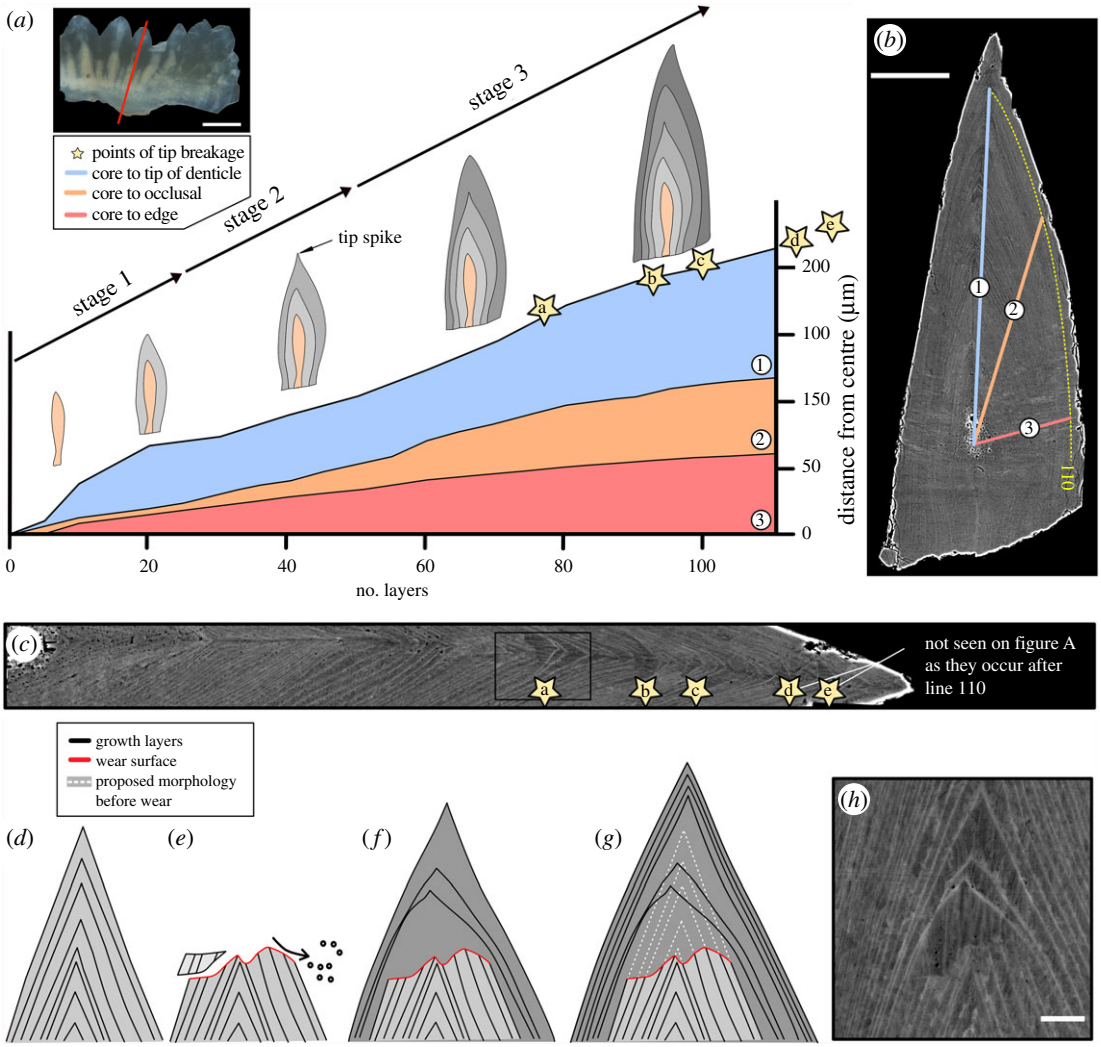

Figure 1. Reconstruction of growth dynamics obtained from a histological thin section of *Ozarkodina confluens*. (*a*) Morphological change calibrated with individual growth layers (lamellae of the crown tissue). (*b*) Composite BSE images of polished thin section (scale bar 50 µm) through the conodont element outlining three transects along which lamellae were counted. (*c*) Episodes of wear recorded as tip breakages. (*d*–*g*) Reconstruction of wear followed by repair of the damaged element. (*h*) BSE image of wear surface (scale bar 5 µm). (Online version in colour.)

in terms of element uptake, the analysis has been performed for all three stages as well as for stages 2 and 3 only. Details of the analyses are presented in [24].

3. Results

(a) Growth dynamics

An episode of growth refers to the accretion of an individual lamella to the outermost surface of the element. Episodes of wear are defined as areas in which the lamellar tissue can clearly be seen truncated or removed and are capped with further growth. They are interpreted here as wear rather than abrupt breakage because of their jagged shape and because these surfaces have been shown before to continue across multiple denticles [11,12,26].

(i) Normal specimen

A total of 137 lamellae could be described (figure 1*a*). Towards the outer edge of the element, however, lamellae were not clearly distinguishable. Therefore, we will only refer to the first 110 layers (boundary defined on figure 1*b*). Three transects originating from the centre of the element were drawn across the crown, representing: (i) the growth axis, (ii) the direction perpendicular to the occlusal side of the element, and (iii) an axis perpendicular to the lamellae. The thickness of lamellae was recorded along these three transects, allowing the characterization of changes in the direction of growth during ontogenesis [24].

Individual lamellae can be as thin as 400 nm and are represented as pairs of dark and light bands. The thicknesses of dark bands vary between 159 nm and 9.5 µm, with peak thicknesses recorded within areas of tip repair (mean = 779 nm, $\sigma = 1$ µm). Lighter bands show less variation in thickness, ranging from *ca* 165 nm to 551 nm (mean = 294 nm, $\sigma = 83$ nm). The thickness range of the layers fluctuates throughout the sample but appears to follow an overall trend of narrowing towards the edge of the specimen, possibly reflecting a slowing of growth with age (determinate growth). Within the first 110 layers of growth, three morphological stages can be distinguished (figure 1*a*). They are defined by changes in tip and whole element morphology. The first stage of growth is a thin elongated element, with vertical growth (core to tip) being dominant (core to layer 23). The second stage shows a small increase in growth towards the occlusal edge of the element (figure 1*a*). Within this stage, an elongated spike on the tip of denticle is formed

Downloaded from https://royalsocietypublishing.org/ on 09 November 2023

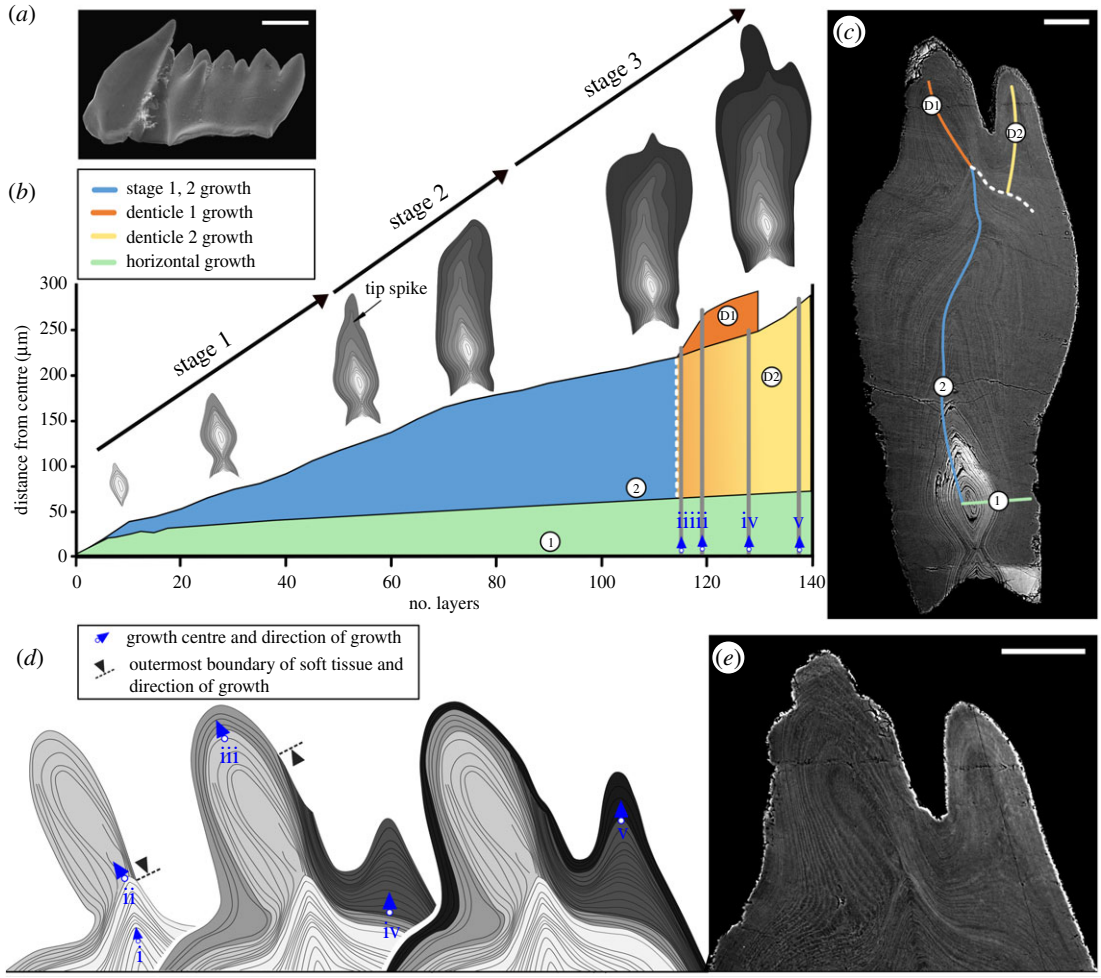

Figure 2. Growth dynamics and ontogenetic development of pathologically developed *Ozarkodina confluens*. (*a*) Overview of the specimen in scanning electron microscopy (SEM) (scale bar 200 µm). (*b*) Morphological change calibrated with individual growth layers (lamellae of the crown tissue). The graph represents growth rates during life, ontogenetic development, preference of growth direction during life, and the areas in which growth centres could be identified (growth centre (i) corresponds to the base of the growth axis). (*c*) Composite BSE image of polished thin section (scale bar 50 µm). (*d*) Reconstruction of the development of growth centres (ii–v) and the inferred extent soft tissue over the surface of the element. (*e*) BSE image of malformed denticles (D1 and D2; scale bar 50 µm). (Online version in colour.)

(layers 23–48). It is at the end of this stage (layers 69–73) that the first occurrence of tip wear is recorded. In the third stage, the element shows preferential vertical growth from the base of the element and distinctive thickening of the lamellar tissue towards the occlusal surface.

Tip wear. A sequence of five wear surfaces has been identified within the element (figure 1*c*). The first tip wear occurs at the 65th layer (seen here only in the normally formed element). Between 13 and 16 layers of the tip have been removed from these areas, creating an irregular surface that truncates the lamellar tissues. All these surfaces show a systematic repair of the damaged tips: (i) the area of wear is capped by a single layer of growth, (ii) 'original' morphology is restored within 2–3 layers, and (iii) 10–13 layers are concentrically accreted around the entire element before the cycle is repeated (figure 1*d*).

(ii) Pathological specimen

Two deformations can be seen on the specimen surface (figure 2*a*): the large, distorted cusp and the duplicated denticle that grows on one side of the blade. Owing to the overall shape distortion and the lack of detectable wear, it is difficult to determine the occlusal surface of the element. In the histological section, the three growth stages described above can also be seen with similar relative durations (figure 2*b*): (i) a preference for vertical growth is seen within the first 15–20 lamellae, (ii) followed by a similar development of a spike on the tip of the element in layers 35–45 [24]. It is at this stage that the direction of growth begins to shift out of the axis (layers 50–75). Subsequently, the orientation of the tip is tentatively corrected (layers 70–110) and 'rounding' of the element occurs with amplified growth on both sides of the blade's surface. Following this boundary, a sudden morphological change occurs within the element, marked by the development of an asymmetrical, tilted denticle (denticle D1 in figure 2*c*). The direction of growth varies with respect to the cutting plane, which results in difficulties in deciphering the sequence of growth. Bundles of conformably deposited lamellae are used in figure 2*d* to infer intervals of growth from discrete growth centres (i–v). Up to this point (lamella 110), no detectable growth arrest is found and all lamellae are tentatively attributed to a single growth interval. The tilted denticle (D1 in figure 2*c*) is formed by two discrete bundles of lamellae, attributed to growth centres (ii) and (iii). The former bundle terminates on the oral side of the element instead of reaching to the base as is typical for normally developed lamellae. Following the formation of the tilted

Downloaded from https://royalsocietypublishing.org/ on 09 November 2023

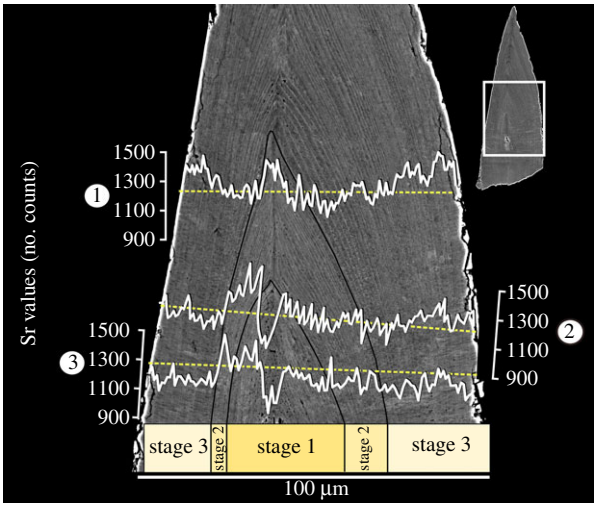

Figure 3. Changes in Sr content within growth stages of *Ozarkodina confluens*. Occlusal side of the element is on the right of the image. (Online version in colour.)

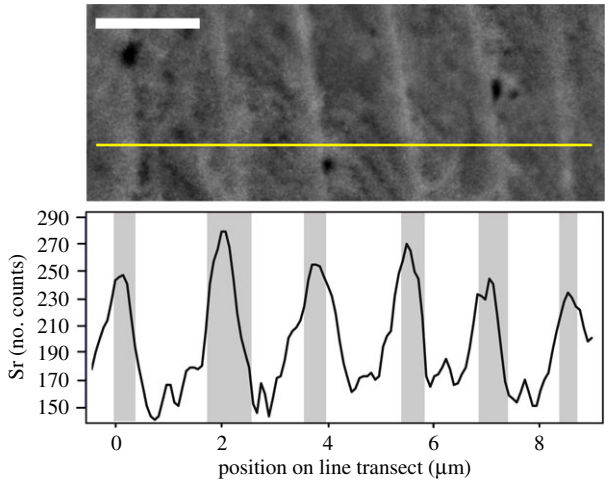

Figure 4. Sr concentration fluctuations recorded within individual lamellae of *Ozarkodina confluens*. Horizontal line in the upper half of the image represents the location of the high-resolution EDX line transect. Scale bar 2 µm. (Online version in colour.)

denticle D1, a new growth centre (iv) appeared on the side of the blade, leading to the development of an out-of-axis denticle (D2 in figure 2*c*). The bundle of lamellae generated from this centre also terminates on the oral surface, on the side of denticle D1. Finally, the entire surface of the element is enveloped by lamellae growing from a new (v) growth centre, which continued to expand denticle D2. Beyond this point, lamellae at the edge of the section could not be resolved.

(b) Chemical composition

Major elements present in crown tissues (Sr, F, Mg, O, Ca, P, Na) have been analysed in the normally developed element to identify the source of differences in the BSE signal making individual lamellae visible. Of these elements, Sr has been identified as systematically changing between light and dark bands as well as across the entire conodont element. The effect of diagenesis on Sr content in conodont bioapatite is not fully understood, but comparisons with other proxies and the distribution of other elements indicate that conodont lamellar tissue is the least susceptible to diagenetic alteration among all bioapatites [27]. The risk of diagenesis in our study was mitigated by using conodonts which had never undergone burial or hydrothermal diagenesis (Conodont Alteration Index 1).

(i) Distribution across the element

Three horizontal EDX line scans were conducted across the element. The lowest Sr concentration is found in the centre of the element (mean 1225 counts, minimum 942, $\sigma = 135$) and it increases towards the outer edge of stage 2 growth, where it peaks (mean 1262 counts, minimum 1065, $\sigma = 105$; figure 3). Growth stage 1 shows an overall increase in Sr counts from the growth axis, followed by higher on average values within the second stage, decreasing towards the boundary with growth stage 3. A drastic drop is observed at this boundary, followed by a gradual increase in Sr content towards the edge of the element [24]. Average Sr content differed significantly between the lamellar tissues building growth stages 2 and 3 ($p = 0.001$) and the model incorporating the growth stage and the side of the element (occlusal versus non-occlusal) had the strongest support (Akaike's information criteria $= -774.06$, Bayesian information criteria $= -755.25$, $p = 0.0008$) compared with models incorporating only the growth stage ($p = 0.0007$) or the side ($p = 0.02$). These differences were consistent even though there was considerable variability between the transects [24], reflecting different growth rates in different parts along the height of the element. The models accounted for this variability, treating them as random effects. These differences were also significant in spite of the growth rate being higher on the occlusal side compared to the non-occlusal side, which was associated with thicker lamellae and higher noise in Sr counts (figure 3).

(ii) Distribution in lamellae

A short, high-resolution line scan (figure 4; [24]) was conducted in areas of the element where individual layers are easily identified. This transect reveals that Sr concentrations are consistently higher in light bands and lower in the dark (figure 4). These peaks of Sr concentration have been identified within layers as thin as *ca* 500 nm, but the most robust results were obtained in layers greater than 1 µm thick.

4. Discussion

(a) Growth mechanism

The normally developed conodont reveals clear cycles of growth, illustrated by the reoccurring episodic damage followed by systematic repair (figure 1). Episodes of wear only occur from the 69th growth layer and minor and major growth lines that have been discussed by other authors [12,15] have not been observed in this study. It is possible that conodonts exhibited continuous growth during their first two phases of growth (as proposed for type III growth characterizing this species [13]), before transitioning to a discontinuous model when the feeding function of the elements began. Periodic growth is in agreement with previous studies [14,15,17,26]. Normally developed *O. confluens* recorded at least five episodes of function marked by wear (figure 1*a*,*c*). The distribution of length of elements of the same species revealed at least 3.5 size classes [17], corresponding to discrete growth stages. In coniform species, 9–16 major increments (bundles of layers) were found [15],

Downloaded from https://royalsocietypublishing.org/ on 09 November 2023

but it is not clear whether these bundles are of the same origin as the bundles seen here in *O. confluens*. This periodicity may not be universal in all euconodonts as it could not be found in multiple Devonian species [16].

In the normally developed conodont, growth after each episode of wear continued along the same axis, but the pathological specimen illustrates that: (i) it could also be driven to deviate from the growth axis and (ii) new growth centre could be started outside of this axis (polyaxial mode of growth [10]). This, together with periodic growth, supports periodic retraction to the epidermis and development of a new growth centre after each episode of function [11,18].

In normally developed elements, lamellae extend over the entire outermost surface of the element and commonly connect with their corresponding layers of the basal tissue [12]. The pathological specimen illustrates that lamellae can also come to a stop at the surface of the element. This has been only observed in lamellae bundles developed from a misplaced growth centre. As this happened at a stage in which the element reached its mature size and its shape was distorted, it is conceivable that lamellae which did not reach the base of the element were secreted in a position where the element could not be fully retracted into the epidermis.

(b) Changes of the life and feeding habit during ontogeny

Certain minor elements (e.g. Sr, fluorine and sodium) are incorporated *in vivo* in apatite forming hard tissues [28]. The levels of Sr shown here reveal consistent patterns across the three stages of element growth (figure 3). Sr uptake in skeletal tissues is primarily determined by the concentration and mobility of alkaline earth metals in the water and positively correlated with its temperature [2]. Secondly, it is influenced by the diet. Higher Sr content seen within the second growth stage, followed by a substantial decrease at the boundary between growth stages 2 and 3, may imply that *O. confluens* (i) migrated in its early life across a temperature gradient in the water column or over distances sufficient to reflect the small-scale Sr variability in the ocean [29], or (ii) changed its food base from Sr-richer to Sr-poorer during ontogeny. Vertical migration can be excluded based on the sedimentological data [22]. In trophic chains, Sr in skeletal tissues is increasingly depleted relative to calcium with each transition to a higher level [28]. We suggest that, considering the lack of wear at growth stage 2, *O. confluens* only started mechanical digestion in growth stage 3. In the normally developed specimen, stage 2 ended with the deposition of the 49th lamella. Although the duration of a single apposition episode is unknown, it has been tentatively proposed to be 1 day [15,16,30]. It is unlikely that feeding from an endogenous source such as a yolk sac would last until such a late phase of development.

Compared to, e.g. platform elements, those of *O. confluens* has one of the simplest developmental patterns, with growth centres added along a single axis and process extension by marginal accretion [13]. Nonetheless, anisometric growth can be traced in its cross-sectional morphology, similarly to other conodont species [15,16,26]. The change was interpreted by previous authors as the transition from the juvenile to the adult phase. The presence of a radically different morphology in the earliest growth phase of some species has been proposed to mark the larval stage [19]. Metamorphosis in isolated skeletal tissues can be inferred only based on evidence of the feeding style. The combined record of chemical composition, wear and morphology suggests that conodonts may have fed on low trophic levels and without detectable mechanical digestion early in life, followed by a predatory or scavenger mode of life in growth stage 3, when elements were developed enough to facilitate mechanical digestion. This mature stage was the basis for previous interpretations of the dental function of conodont elements [5,6].

(c) Structure of the lamellae

Descriptions of lamellae in conodont crown tissues vary widely between studies, owing to the great variation of their thickness between ontogenetic stages and taxa [12]. Thicknesses between 1.5 and 5 µm are most commonly reported [15,16,30,31], but values up to 77 µm have been found [12], which can be partly attributed to cutting effects. Lamellae consist of parallel crystallites normal to the growth surface [7,13] and their boundaries, appearing dark in optical thin sections, are accentuated by a higher organic content (not observed within this study) [12]. Three to four interlamellar striations parallel to lamellae boundaries have been proposed [12]. Among other studies, only [15] observed a subdivision of growth layers in the form of minor (1.5–2.5 µm) and major (12 –21.5 µm) increments. Internal inhomogeneity within lamellae has been identified in transmission electron microscopy samples as rhythmic changes in the sizes of (nano)crystal layers [29]. In our study, BSE images did not allow discerning internal subdivision of lamellae beyond the light and dark bands (figure 4). The application of this method to other species should allow for a more reproducible definition of an individual lamella in quantitative growth analyses.

5. Conclusion

We used dental organs of *O. confluens* as a model of euconodont growth. Three phases can be distinguished during their ontogeny. The last phase (maturity) is characterized by periodic (at least five episodes) wear of the occlusal area of the element and repair by the addition of new growth centres. Growth by the addition of new centres is manifested in the pathological specimens where they are placed out of the normal growth axis. The three ontogenetic stages differ in the Sr concentration in the corresponding tissue. Also, individual growth layers are distinguished by periodic changes in their Sr content [32], which appears to underpin their visibility in BSE imaging. Our results support the model of periodic engulfment of elements in the epidermis and addition of new growth centres [11,12,18], as well as a change in life or feeding habit and potential metamorphosis [19] before the onset of scavenger or predator type of feeding in adult animals.

Data accessibility. Supplementary data and figures available in the Dryad Data Repository: http://dx.doi.org/10.5061/dryad.5q9q697 [24].

Authors' contributions. B.S., E.J. and M.B. designed the study; B.S. and M.G. prepared histological sections and carried out the analyses; B.S., M.G., M.B. and E.J. interpreted the data; B.S. and E.J. wrote the paper. All the authors gave their final approval for publication.

Competing interests. We declare we have no competing interests.

Funding. The study was supported by the Deutsche Forschungsgemeinschaft (grant no. Ja 2718/1-1). Material from the Swedish

Downloaded from https://royalsocietypublishing.org/ on 09 November 2023

Museum of Natural History was made accessible thanks to grant no. SE-TAF-5040 from SYNTHESYS to E.J., which is financed by the European Community–Research Infrastructure Action under the Seventh Framework Programme (FP7/2007–2013).

Acknowledgements. We thank V. Vajda, T. Mörs and Ch. Skovsted for providing access to the pathological specimen hosted at the Swedish Museum of Natural History. B. Leipner-Mata helped in thin section preparation and Ch. Schulbert in SEM work.

References

1. Donoghue PCJ, Sansom IJ. 2002 Origin and early evolution of vertebrate skeletonization. *Microsc. Res. Tech.* **59**, 352–372. (doi:10.1002/jemt.10217)
2. Murdock DJE, Dong X-P, Repetski JE, Marone F, Stampanoni M, Donoghue PCJ. 2013 The origin of conodonts and of vertebrate mineralized skeletons. *Nature* **502**, 546–549. (doi:10.1038/nature12645)
3. Briggs DEG, Clarkson ENK, Aldridge RJ. 1983 The conodont animal. *Lethaia* **16**, 1–14. (doi:10.1111/j.1502-3931.1983.tb01993.x)
4. Gabbott SE, Aldridge RJ, Theron JN. 1995 A giant conodont with preserved muscle tissue from the Upper Ordovician of South Africa. *Nature* **374**, 800–803.
5. Purnell MA. 1993 Feeding mechanisms in conodonts and the function of the earliest vertebrate hard tissues. *Geology* **21**, 375–377.
6. Purnell MA. 1995 Microwear on conodont elements and macrophagy in the first vertebrates. *Nature* **374**, 798–800.
7. Donoghue PCJ. 2001 Microstructural variation in conodont enamel is a functional adaptation. *Proc. R. Soc. Lond. B* **268**, 1691–1698. (doi:10.1098/rspb.2001.1728)
8. Jones D, Evans AR, Siu KKW, Rayfield EJ, Donoghue PCJ. 2012 The sharpest tools in the box? Quantitative analysis of conodont element functional morphology. *Proc. R. Soc. B* **279**, 2849–2854. (doi:10.1098/rspb.2012.0147)
9. Martínez-Pérez C, Rayfield EJ, Purnell MA, Donoghue PCJ. 2014 Finite element, occlusal, microwear and microstructural analyses indicate that conodont microstructure is adapted to dental function. *Palaeontology* **57**, 1059–1066. (doi:10.1111/pala.12102)
10. Hass WH. 1941 Morphology of conodonts. *J. Paleontol.* **15**, 71–81.
11. Donoghue PCJ, Purnell MA. 1999 Growth, function, and the conodont fossil record. *Geology* **27**, 251–254.
12. Müller KJ, Nogami Y. 1971 Über den Feinbau der Conodonten. *Mem. Faculty Sci., Kyoto Uni. Series Geol. and Mineral.* **38**, 1–87.
13. Donoghue PCJ. 1998 Growth and patterning in the conodont skeleton. *Phil. Trans. R. Soc. Lond. B* **353**, 633–666. (doi:10.1098/rstb.1998.0231)
14. Zhang S, Aldridge RJ, Donoghue PCJ. 1997 An Early Triassic conodont with periodic growth? *J. Micropalaeontol.* **16**, 65–72. (doi:10.1144/jm.16.1.65)
15. Armstrong HA, Smith CJ. 2001 Growth patterns in euconodont crown enamel: implications for life history and mode-of-life reconstruction in the earliest vertebrates. *Proc. R. Soc. Lond. B* **268**, 815–820. (doi:10.1098/rspb.2001.1591)
16. Dzik J. 2008 Evolution of morphogenesis in 360-million-year-old conodont chordates calibrated in days. *Evol. Dev.* **10**, 769–777. (doi:10.1111/j.1525-142X.2008.00291.x)
17. Jeppsson L. 1976 Autecology of Late Silurian conodonts. In *Conodont paleoecology* (ed. CR Barnes), pp. 105-118. Waterloo, Canada: Geological Association of Canada.
18. Bengtson S. 1976 The structure of some Middle Cambrian conodonts, and the early evolution of conodont structure and function. *Lethaia* **9**, 185–206. (doi:10.1111/j.1502-3931.1976.tb00966.x)
19. Dzik J. 2006 The Famennian 'Golden Age' of conodonts and ammonoids in the Polish part of the Variscan sea. *Palaeontol. Polonica* **63**, 1–360.
20. Dzik J. 2000 The origin of the mineral skeleton in chordates. In *Evolutionary biology* (ed. MK Hecht), pp. 105-154. New York, NY: Kluwer.
21. Purnell MA, Donoghue PCJ, Aldridge RJ. 2000 Orientation and anatomical notation in conodonts. *J. Paleontol.* **74**, 113–122.
22. Jarochowska E, Bremer O, Heidlas D, Pröpster S, Vandenbroucke TR, Munnecke A. 2016 End-Wenlock terminal Mulde carbon isotope excursion in Gotland, Sweden: integration of stratigraphy and taphonomy for correlations across restricted facies and specialized faunas. *Palaeogeogr. Palaeoclimatol. Palaeoecol.* **457**, 304–322.
23. Martínez-Pérez C, Plasencia P, Jones D, Kolar-Jurkovšek T, Sha J, Botella H, Donoghue PC. 2014 There is no general model for occlusal kinematics in conodonts. *Lethaia* **47**, 547–555.
24. Shirley B, Grohganz M, Bestmann M, Jarochowska E. 2018 Data from: Wear, tear and systematic repair: testing models of growth dynamics in conodonts with high-resolution imaging. Dryad Digital Repository. (http://dx.doi.org/10.5061/dryad.5q9q697)
25. Bates D, Maechler M, Bolker B, Walker S. 2015 Fitting linear mixed-effects models using lme4. *J. Stat. Software* **67**, 1–48. (doi:10.18637/jss.v067.i01)
26. Mazza M, Martínez-Pérez C. 2016 Evolutionary convergence in conodonts revealed by synchrotron-based tomographic microscopy. *Palaeontol. Electronica.* **19**, 1. (doi:10.26879/681)
27. Balter V, Lécuyer C. 2010 Determination of Sr and Ba partition coefficients between apatite from fish (*Sparus aurata*) and seawater: the influence of temperature. *Geochim. Cosmochim. Acta* **74**, 3449–3458. (doi:10.1016/j.gca.2010.03.015)
28. Reynard B, Balter V. 2014 Trace elements and their isotopes in bones and teeth: diet, environments, diagenesis, and dating of archeological and paleontological samples. *Palaeogeogr. Palaeoclimatol. Palaeoecol.* **416**(Suppl. C), 4–16. (doi:10.1016/j.palaeo.2014.07.038)
29. de Villiers S. 1999 Seawater strontium and Sr/Ca variability in the Atlantic and Pacific oceans. *Earth Planet. Sci. Lett.* **171**, 623–634. (doi:10.1016/S0012-821X(99)00174-0)
30. Świś P. 2018 Population dynamics of the Late Devonian conodont *Alternognathus* calibrated in days. *Hist. Biol.* **16**, 1–9. (doi:10.1080/08912963.2018.1427088)
31. Pietzner H, Vahl J, Werner H, Ziegler W. 1968 Zur chemischen Zusammensetzung und Mikromorphologie der Conodonten. *Palaeontographica Abteilung A* **128**, 115–152.
32. Zhuravlev AV, Shevchuk SS. 2017 Strontium distribution in Upper Devonian conodont elements: a palaeobiological proxy. *Rivista Italiana di Paleontologia e Stratigrafia* **123**, 203–202.